(124) Wagenseil, J. E.; Mecham, R. P. *Physiol. Rev.* **2009**, *89*, 957.
(125) Chaudhuri, O.; Mooney, D. J. *Nat. Mater.* **2012**, *11*, 568.
(126) Yim, E. K. F.; Pang, S. W.; Leong, K. W. *Exp. Cell Res.* **2007**, *313*, 1820.
(127) Dalby, M. J.; McCloy, D.; Robertson, M.; Agheli, H.; Sutherland, D.; Affrossman, S.; Oreffo, R. O. C. *Biomaterials* **2006**, *27*, 2980.
(128) Silva, G. A.; Czeisler, C.; Niece, K. L.; Beniash, E.; Harrington, D. A.; Kessler, J. A.; Stupp, S. I. *Science* **2004**, *303*, 1352.
(129) Curtis, A.; Wilkinson, C. *Trends Biotechnol.* **2001**, *19*, 97.
(130) Abrams, G. A.; Goodman, S. L.; Nealey, P. F.; Franco, M.; Murphy, C. J. *Cell Tissue Res.* **2000**, *299*, 39.
(131) Wan, L. Q.; Kang, S. M.; Eng, G.; Grayson, W. L.; Lu, X. L.; Huo, B.; Gimble, J.; Guo, X. E.; Mow, V. C.; Vunjak-Novakovic, G. *Integr. Biol.* **2010**, *2*, 346.
(132) Tang, J.; Peng, R.; Ding, J. *Biomaterials* **2010**, *31*, 2470.
(133) Tay, C. Y.; Yu, H. Y.; Pal, M.; Leong, W. S.; Tan, N. S.; Ng, K. W.; Leong, D. T.; Tan, L. P. *Exp. Cell Res.* **2010**, *316*, 1159.
(134) Ruiz, A.; Buzanska, L.; Gilliland, D.; Rauscher, H.; Sirghi, L.; Sobanski, T.; Zychowicz, M.; Ceriotti, L.; Bretagnol, F.; Coecke, S.; Colpo, P.; Ross, F. *Biomaterials* **2008**, *29*, 4766.
(135) Beduer, A.; Vieu, C.; Arnauduc, F.; Sol, J. C.; Loubinoux, I.; Vaysse, L. *Biomaterials* **2012**, *33*, 504.
(136) Biehl, J. K.; Yamanaka, S.; Desai, T. A.; Boheler, K. R.; Russell, B. *Dev. Dyn.* **2009**, *238*, 1964.
(137) Luo, W.; Jones, S. R.; Yousaf, M. N. *Langmuir* **2008**, *24*, 12129.
(138) Connelly, J. T.; Gautrot, J. E.; Trappmann, B.; Tan, D. W. M.; Donati, G.; Huck, W. T. S.; Watt, F. M. *Nat. Cell Biol.* **2010**, *12*, 711.
(139) Song, W.; Kawazoe, N.; Chen, G. P. *J. Nanomater.* **2011**, No. 265251.
(140) Wang, W. J.; Itaka, K.; Ohba, S.; Nishiyama, N.; Chung, U. I.; Yamasaki, Y.; Kataoka, K. *Biomaterials* **2009**, *30*, 2705.
(141) Peerani, R.; Rao, B. M.; Bauwens, C.; Yin, T.; Wood, G. A.; Nagy, A.; Kumacheva, E.; Zandstra, P. W. *EMBO J.* **2007**, *26*, 4744.
(142) Bauwens, C. L.; Peerani, R.; Niebruegge, S.; Woodhouse, K. A.; Kumacheva, E.; Husain, M.; Zandstra, P. W. *Stem Cells* **2008**, *26*, 2300.
(143) Niebruegge, S.; Bauwens, C. L.; Peerani, R.; Thavandiran, N.; Masse, S.; Sevaptisidis, E.; Nanthakumar, K.; Woodhouse, K.; Husain, M.; Kumacheva, E.; Zandstra, P. W. *Biotechnol. Bioeng.* **2009**, *102*, 493.
(144) Higuchi, A.; Sugiyama, K.; Yoon, B. O.; Sakurai, M.; Hara, M.; Sumita, M.; Sugawara, S.; Shirai, T. *Biomaterials* **2003**, *24*, 3235.
(145) Higuchi, A.; Aoki, N.; Yamamoto, T.; Gomei, Y.; Egashira, S.; Matsuoka, Y.; Miyazaki, T.; Fukushima, H.; Jyujyoji, S.; Natori, S. H. *Biomacromolecules* **2006**, *7*, 1083.
(146) Higuchi, A.; Yamamoto, T.; Sugiyama, K.; Hayashi, S.; Tak, T. M.; Nakagawa, T. *Biomacromolecules* **2005**, *6*, 691.
(147) Myllymaa, S.; Kaivosoja, E.; Myllymaa, K.; Sillat, T.; Korhonen, H.; Lappalainen, R.; Konttinen, Y. T. *J. Mater. Sci: Mater. Med.* **2010**, *21*, 329.
(148) Peng, R.; Yao, X.; Ding, J. D. *Biomaterials* **2011**, *32*, 8048.
(149) Song, W.; Lu, H. X.; Kawazoe, N.; Chen, G. P. *Langmuir* **2011**, *27*, 6155.
(150) Connelly, J. T.; Mishra, A.; Gautrot, J. E.; Watt, F. M. *PLoS One* **2011**, *6*, No. e27259.
(151) Seo, C. H.; Furukawa, K.; Suzuki, Y.; Kasagi, N.; Ichiki, T.; Ushida, T. *Macromol. Biosci.* **2011**, *11*, 938.
(152) Kurpinski, K.; Chu, J.; Hashi, C.; Li, S. *Proc. Natl. Acad. Sci. U.S.A.* **2006**, *103*, 16095.
(153) Recknor, J. B.; Sakaguchi, D. S.; Mallapragada, S. K. *Biomaterials* **2006**, *27*, 4098.
(154) D'Angelo, F.; Armentano, I.; Mattioli, S.; Crispoltoni, L.; Tiribuzi, R.; Cerulli, G. G.; Palmerini, C. A.; Kenny, J. M.; Martino, S.; Orlacchio, A. *Eur. Cells Mater.* **2010**, *20*, 231.
(155) Tuleuova, N.; Lee, J. Y.; Lee, J.; Ramanculov, E.; Zern, M. A.; Revzin, A. *Biomaterials* **2010**, *31*, 9221.
(156) Li, X.; Chu, J. L.; Wang, A. J.; Zhu, Y. Q.; Chu, W. K.; Yang, L.; Li, S. *PLoS One* **2011**, *6*, No. e26029.
(157) Niklason, L. E.; Gao, J.; Abbott, W. M.; Hirschi, K. K.; Houser, S.; Marini, R.; Langer, R. *Science* **1999**, *284*, 489.
(158) Kim, B. S.; Nikolovski, J.; Bonadio, J.; Mooney, D. J. *Nat. Biotechnol.* **1999**, *17*, 979.
(159) Hamilton, D. W.; Maul, T. M.; Vorp, D. A. *Tissue Eng.* **2004**, *10*, 361.
(160) Canham, P. B.; Mullin, K. *J. Microsc.* **1978**, *114*, 307.
(161) Walmsley, J. G.; Campling, M. R.; Chertkow, H. M. *Stroke* **1983**, *14*, 781.
(162) Paralkar, V. M.; Vukicevic, S.; Reddi, A. H. *Dev. Biol.* **1991**, *143*, 303.
(163) Silver, J.; Miller, J. H. *Nat. Rev. Neurosci.* **2004**, *5*, 146.
(164) Levenberg, S.; Huang, N. F.; Lavik, E.; Rogers, A. B.; Itskovitz-Eldor, J.; Langer, R. *Proc. Natl. Acad. Sci. U.S.A.* **2003**, *100*, 12741.
(165) Park, K. I.; Teng, Y. D.; Snyder, E. Y. *Nat. Biotechnol.* **2002**, *20*, 1111.
(166) Teng, Y. D.; Lavik, E. B.; Qu, X.; Park, K. I.; Ourednik, J.; Zurakowski, D.; Langer, R.; Snyder, E. Y. *Proc. Natl. Acad. Sci. U.S.A.* **2002**, *99*, 3024.
(167) Beduer, A.; Vaysse, L.; Flahaut, E.; Seichepine, F.; Loubinoux, I.; Vieu, C. *Microelectron. Eng.* **2011**, *88*, 1668.
(168) Lietz, M.; Dreesmann, L.; Hoss, M.; Oberhoffner, S.; Schlosshauer, B. *Biomaterials* **2006**, *27*, 1425.
(169) Morelli, S.; Salerno, S.; Piscioneri, A.; Papenburg, B. J.; Di Vito, A.; Giusi, G.; Canonaco, M.; Stamatialis, D.; Drioli, E.; De Bartolo, L. *Biomaterials* **2010**, *31*, 7000.
(170) Mahoney, M. J.; Chen, R. R.; Tan, J.; Saltzman, W. M. *Biomaterials* **2005**, *26*, 771.
(171) Miller, C.; Shanks, H.; Witt, A.; Rutkowski, G.; Mallapragada, S. *Biomaterials* **2001**, *22*, 1263.
(172) Hosseinkhani, H.; Hosseinkhani, M.; Tian, F.; Kobayashi, H.; Tabata, Y. *Biomaterials* **2006**, *27*, 4079.
(173) Ma, Z. W.; Kotaki, M.; Inai, R.; Ramakrishna, S. *Tissue Eng.* **2005**, *11*, 101.
(174) Padin-Iruegas, M. E.; Misao, Y.; Davis, M. E.; Segers, V. F. M.; Esposito, G.; Tokunou, T.; Urbanek, K.; Hosoda, T.; Rota, M.; Anversa, P.; Leri, A.; Lee, T.; Kajstura, J. *Circulation* **2009**, *120*, 876.
(175) Gelain, F.; Bottai, D.; Vescovi, A.; Zhang, S. *PLoS One* **2006**, *1*, No. e119.
(176) Hosseinkhani, H.; Hosseinkhani, M.; Kobayashi, H. *Biomed. Mater.* **2006**, *1*, 8.
(177) Galler, K. M.; Cavender, A.; Yuwono, V.; Dong, H.; Shi, S. T.; Schmalz, G.; Hartgerink, J. D.; D'Souza, R. N. *Tissue Eng., Part A* **2008**, *14*, 2051.
(178) Guo, H. D.; Cui, G. H.; Wang, H. J.; Tan, Y. Z. *Biochem. Biophys. Res. Commun.* **2010**, *399*, 42.
(179) Cooke, M. J.; Zahir, T.; Phillips, S. R.; Shah, D. S.; Athey, D.; Lakey, J. H.; Shoichet, M. S.; Przyborski, S. A. *J. Biomed. Mater. Res., Part A* **2010**, *93A*, 824.
(180) Anderson, J. M.; Kushwaha, M.; Tambralli, A.; Bellis, S. L.; Camata, R. P.; Jun, H. W. *Biomacromolecules* **2009**, *10*, 2935.
(181) Bakota, E. L.; Wang, Y.; Danesh, F. R.; Hartgerink, J. D. *Biomacromolecules* **2011**, *12*, 1651.
(182) Lim, S. H.; Liu, X. Y.; Song, H. J.; Yarema, K. J.; Mao, H. Q. *Biomaterials* **2010**, *31*, 9031.
(183) Wang, Y.; Bakota, E.; Chang, B. H.; Entman, M.; Hartgerink, J. D.; Danesh, F. R. *J. Am. Soc. Nephrol.* **2011**, *22*, 704.
(184) Galler, K. M.; Cavender, A.; Yuwono, V.; Dong, H.; Shi, S.; Schmalz, G.; Hartgerink, J. D.; D'Souza, R. N. *Tissue Eng., Part A* **2008**, *14*, 2051.
(185) Hughes, C. S.; Postovit, L. M.; Lajoie, G. A. *Proteomics* **2010**, *10*, 1886.
(186) Uemura, M.; Refaat, M. M.; Shinoyama, M.; Hayashi, H.; Hashimoto, N.; Takahashi, J. *J. Neurosci. Res.* **2010**, *88*, 542.
(187) Lei, X.; Liu, B.; Wu, J.; Lu, Y.; Yang, Y. *Anat. Rec.* **2011**, *294*, 1525.
(188) Kleinman, H. K.; Martin, G. R. *Semin. Cancer Biol.* **2005**, *15*, 378.
(189) Blakeney, B. A.; Tambralli, A.; Anderson, J. M.; Andukuri, A.; Lim, D. J.; Dean, D. R.; Jun, H. W. *Biomaterials* **2011**, *32*, 1583.

(190) El-Newehy, M. H.; Al-Deyab, S. S.; Kenawy, E. R.; Abdel-Megeed, A. *Fiber Polym.* **2012**, *13*, 709.
(191) Shih, Y. R. V.; Chen, C. N.; Tsai, S. W.; Wang, Y. J.; Lee, O. K. *Stem Cells* **2006**, *24*, 2391.
(192) Ko, E. K.; Jeong, S. I.; Rim, N. G.; Lee, Y. M.; Shin, H.; Lee, B. K. *Tissue Eng., Part A* **2008**, *14*, 2105.
(193) Sefcik, L. S.; Neal, R. A.; Kaszuba, S. N.; Parker, A. M.; Katz, A. J.; Ogle, R. C.; Botchwey, E. A. *J. Tissue Eng. Regener. Med.* **2008**, *2*, 210.
(194) Schofer, M. D.; Boudriot, U.; Leifeld, I.; Sutterlin, R. I.; Rudisile, M.; Wendorff, J. H.; Greiner, A.; Paletta, J. R. J.; Fuchs-Winkelmann, S. *TheScientificWorldJournal* **2009**, *9*, 118.
(195) Seyedjafari, E.; Soleimani, M.; Ghaemi, N.; Shabani, I. *Biomacromolecules* **2010**, *11*, 3118.
(196) Chen, J. P.; Chang, Y. S. *Colloids Surf., B* **2011**, *86*, 169.
(197) Shabani, I.; Haddadi-Asl, V.; Soleimani, M.; Seyedjafari, E.; Babaeijandaghi, F.; Ahmadbeigi, N. *Tissue Eng., Part A* **2011**, *17*, 1209.
(198) Xin, X. J.; Hussain, M.; Mao, J. J. *Biomaterials* **2007**, *28*, 316.
(199) Baker, B. M.; Shah, R. P.; Huang, A. H.; Mauck, R. L. *Tissue Eng., Part A* **2011**, *17*, 1445.
(200) Yin, Z.; Chen, X.; Chen, J. L.; Shen, W. L.; Nguyen, T. M. H.; Gao, L.; Ouyang, H. W. *Biomaterials* **2010**, *31*, 2163.
(201) Li, W. J.; Tuli, R.; Huang, X.; Laquerriere, P.; Tuan, R. S. *Biomaterials* **2005**, *26*, 5158.
(202) Kolambkar, Y. M.; Peister, A.; Ekaputra, A. K.; Hutmacher, D. W.; Guldberg, R. E. *Tissue Eng., Part A* **2010**, *16*, 3219.
(203) Boudriot, U.; Goetz, B.; Dersch, R.; Greiner, A.; Wendorff, J. H. *Macromol. Symp.* **2005**, *225*, 9.
(204) Schofer, M. D.; Fuchs-Winkelmann, S.; Grabedunkel, C.; Wack, C.; Dersch, R.; Rudisile, M.; Wendorff, J. H.; Greiner, A.; Paletta, J. R. J.; Boudriot, U. *TheScientificWorldJournal* **2008**, *8*, 1269.
(205) Janjanin, S.; Li, W. J.; Morgan, M. T.; Shanti, R. M.; Tuan, R. S. *J. Surg. Res.* **2008**, *149*, 47.
(206) Prabhakaran, M. P.; Venugopal, J. R.; Ramakrishna, S. *Biomaterials* **2009**, *30*, 4996.
(207) Liu, T.; Teng, W. K.; Chan, B. P.; Chew, S. Y. *J. Biomed. Mater. Res., Part A* **2010**, *95*, 276.
(208) Mahairaki, V.; Lim, S. H.; Christopherson, G. T.; Xu, L.; Nasonkin, I.; Yu, C.; Mao, H. Q.; Koliatsos, V. E. *Tissue Eng., Part A* **2011**, *17*, 855.
(209) Wang, J. X.; Ye, R.; Wei, Y. H.; Wang, H. H.; Xu, X. J.; Zhang, F.; Qu, J.; Zuo, B. Q.; Zhang, H. X. *J. Biomed. Mater. Res., Part A* **2012**, *100A*, 632.
(210) Das, H.; Abdulhameed, N.; Joseph, M.; Sakthivel, R.; Mao, H. Q.; Pompili, V. J. *Cell Transplant.* **2009**, *18*, 305.
(211) Ma, K.; Liao, S.; He, L.; Lu, J.; Ramakrishna, S.; Chan, C. K. *Tissue Eng., Part A* **2011**, *17*, 1413.
(212) Hashemi, S. M.; Soleimani, M.; Zargarian, S. S.; Haddadi-Asl, V.; Ahmadbeigi, N.; Soudi, S.; Gheisari, Y.; Hajarizadeh, A.; Mohammadi, Y. *Cells Tissues Organs* **2009**, *190*, 135.
(213) Ghaedi, M.; Soleimani, M.; Shabani, I.; Duan, Y.; Lotfi, A. S. *Cell. Mol. Biol. Lett.* **2012**, *17*, 89.
(214) Zajicova, A.; Pokorna, K.; Lencova, A.; Krulova, M.; Svobodova, E.; Kubinova, S.; Sykova, E.; Pradny, M.; Michalek, J.; Svobodova, J.; Munzarova, M.; Holan, V. *Cell Transplant.* **2010**, *19*, 1281.
(215) Chang, C. H.; Lin, H. Y.; Fang, H. W.; Loo, S. T.; Hung, S. C.; Ho, Y. C.; Chen, C. C.; Lin, F. H.; Liu, H. C. *Artif. Organs* **2008**, *32*, 561.
(216) Hall, B. K.; Miyake, T. *Int. J. Dev. Biol.* **1995**, *39*, 881.
(217) Johnstone, B.; Hering, T. M.; Caplan, A. I.; Goldberg, V. M.; Yoo, J. U. *Exp. Cell Res.* **1998**, *238*, 265.
(218) Dawson, J. I.; Wahl, D. A.; Lanham, S. A.; Kanczler, J. M.; Czernuszka, J. T.; Oreffo, R. O. *Biomaterials* **2008**, *29*, 3105.
(219) Christopherson, G. T.; Song, H.; Mao, H. Q. *Biomaterials* **2009**, *30*, 556.
(220) Bi, Y. M.; Ehirchiou, D.; Kilts, T. M.; Inkson, C. A.; Embree, M. C.; Sonoyama, W.; Li, L.; Leet, A. I.; Seo, B. M.; Zhang, L.; Shi, S. T.; Young, M. F. *Nat. Med.* **2007**, *13*, 1219.
(221) Kannus, P. *Scand. J. Med. Sci. Sports* **2000**, *10*, 312.
(222) Hoffmann, A.; Gross, G. *Int. Orthop.* **2007**, *31*, 791.
(223) Hoffmann, A.; Pelled, G.; Turgeman, G.; Eberle, P.; Zilberman, Y.; Shinar, H.; Keinan-Adamsky, K.; Winkel, A.; Shahab, S.; Navon, G.; Gross, G.; Gazit, D. *J. Clin. Invest.* **2006**, *116*, 940.
(224) Fratzl, P.; Gupta, H. S.; Paschalis, E. P.; Roschger, P. *J. Mater. Chem.* **2004**, *14*, 2115.
(225) Smith, L. A.; Liu, X. H.; Hu, J.; Wang, P.; Ma, P. X. *Tissue Eng., Part A* **2009**, *15*, 1855.
(226) Rohwedel, J.; Guan, K.; Zuschratter, W.; Jin, S.; Ahnert-Hilger, G.; Furst, D.; Fassler, R.; Wobus, A. M. *Dev. Biol.* **1998**, *201*, 167.
(227) Xu, X. Y.; Li, X. T.; Peng, S. W.; Xiao, J. F.; Liu, C.; Fang, G.; Chen, K. C.; Chen, G. Q. *Biomaterials* **2010**, *31*, 3967.
(228) Chen, G. Q.; Wu, Q. *Biomaterials* **2005**, *26*, 6565.
(229) Elsdale, T.; Bard, J. *J. Biol. Chem.* **1972**, *54*, 626.
(230) Orza, A.; Soritau, O.; Olenic, L.; Diudea, M.; Florea, A.; Ciuca, D. R.; Mihu, C.; Casciano, D.; Biris, A. S. *ACS Nano* **2011**, *5*, 4490.

Genomic Basis of Aromatase Excess Syndrome: Recombination- and Replication-Mediated Rearrangements Leading to *CYP19A1* Overexpression

Maki Fukami, Takayoshi Tsuchiya, Heike Vollbach, Kristy A. Brown, Shuji Abe, Shigeyuki Ohtsu, Martin Wabitsch, Henry Burger, Evan R. Simpson, Akihiro Umezawa, Daizou Shihara, Kazuhiko Nakabayashi, Serdar E. Bulun, Makio Shozu, and Tsutomu Ogata*

Context: Genomic rearrangements at 15q21 have been shown to cause overexpression of *CYP19A1* and resultant aromatase excess syndrome (AEXS). However, mutation spectrum, clinical consequences, and underlying mechanisms of these rearrangements remain to be elucidated.

Objective: The aim of the study was to clarify such unsolved matters.

Design, Setting, and Methods: We characterized six new rearrangements and investigated clinical outcome and local genomic environments of these rearrangements and of three previously reported duplications/deletions.

Results: Novel rearrangements included simple duplication involving exons 1–10 of *CYP19A1* and simple and complex rearrangements that presumably generated chimeric genes consisting of the coding region of *CYP19A1* and promoter-associated exons of neighboring genes. Clinical severities were primarily determined by the copy number of *CYP19A1* and the property of the fused promoters. Sequences at the fusion junctions suggested nonallelic homologous recombination, nonhomologous end-joining, and replication-based errors as the underlying mechanisms. The breakpoint-flanking regions were not enriched with GC content, palindromes, noncanonical DNA structures, or known rearrangement-associated motifs. The rearrangements resided in early-replicating segments.

Conclusions: These results indicate that AEXS is caused by duplications involving *CYP19A1* and simple and complex rearrangements that presumably lead to the usage of cryptic promoters of several neighboring genes. Our data support the notion that phenotypes depend on the dosage of *CYP19A1* and the characteristics of the fused promoters. Furthermore, we show that the rearrangements in AEXS are generated by both recombination- and replication-mediated mechanisms, independent of the known rearrangement-inducing DNA features or late-replication timing. Thus, AEXS represents a unique model for human genomic disorders. (***J Clin Endocrinol Metab* 98: E2013–E2021, 2013**)

Aromatase excess syndrome (AEXS; MIM no. 139300) is a rare autosomal dominant disorder that causes prepubertal- or peripubertal-onset gynecomastia, hypogonadotropic hypogonadism, advanced bone age, and short adult height in male patients (1, 2). Female patients are usually asymptomatic, although macromastia, irregular menses, and short stature have been reported in a few individuals (2). AEXS results from excessive expression of the aromatase gene *CYP19A1* on chromosome 15q21.2 (NM_000103) (1). *CYP19A1* comprises 11 noncoding exons 1 that function as tissue-specific promoters (exons I.1, IIa, I.8, I.4, I.5, I.7, 1f, I.2, I.6, I.3, and PII), and nine coding exons (exons 2–10) (3, 4). We and other groups have identified various chromosomal rearrangements at

ISSN Print 0021-972X ISSN Online 1945-7197
Printed in U.S.A.

Received June 13, 2013. Accepted September 19, 2013.
First Published Online September 24, 2013

For editorial see page 4676

* Author affiliations are shown at the bottom of the next page.

Abbreviations: AEXS, aromatase excess syndrome; CGH, comparative genomic hybridization.

15q21 in patients with AEXS (1, 2, 5). These rearrangements included duplications that encompassed seven of the 11 noncoding exons 1 of *CYP19A1* and deletions and inversions that generated chimeric genes consisting of coding exons of *CYP19A1* and promoter-associated exons of neighboring genes. Genotype-phenotype analysis has indicated that clinical severities primarily depend on the functional properties of the fused promoters. These findings provide a novel example of gain-of-function mutations resulting from submicroscopic genomic rearrangements.

Rearrangements in the human genome are known to be generated by recombination-based mechanisms, namely, nonallelic homologous recombination and nonhomologous end-joining, and by replication-based mechanisms (6–9). Of these, nonallelic homologous recombination results from unequal crossover between two homologous sequences, usually on the same but sometimes on different chromosomes (10). Nonallelic homologous recombination accounts for most of the recurrent simple deletions and duplications in the human genome and represents the most common abnormality involved in human genomic disorders (9–11). Nonhomologous end-joining occurs as a result of double-strand DNA breakage and subsequent ligation of the two broken DNA ends (12). Nonhomologous end-joining often underlies nonrecurrent simple deletions associated with short nucleotide stretches at the fusion junctions (9–12). Replication-based mechanisms are caused by aberrant template switching during replication and can produce both simple and complex rearrangements that carry microhomologies at the fusion junctions (8, 9, 13). Previous studies have indicated that nonallelic homologous recombination, nonhomologous end-joining, and replication-based mechanisms are facilitated by various local DNA features including high GC content and palindromes (10, 14–16). Highly similar sequences widely spread in the genome ("repetitive elements"), such as *Alu*, LINE1, and MIR, can mediate the occurrence of genomic rearrangements (12). Non-B structures, ie, DNA conformations that differ from the canonical Watson-Crick right-handed double helix, and specific short sequence motifs and tri/tetranucleotides have also been suggested as local genomic stimulants (14–22). Furthermore, replication timing of each chromosomal region appears to determine the frequency of rearrangements; nonallelic homologous recombination preferentially occurs in DNA segments that replicate in early S phase (early-replicating segments), whereas nonhomologous end-joining and replication-based errors frequently appear in late-replicating segments (23).

At present, the underlying mechanisms of the AEXS-associated rearrangements remain largely unknown. Although sequence analysis of the fusion junctions has indicated that nonallelic homologous recombination and nonhomologous end-joining—and possibly replication-based mechanisms as well—are involved in the formation of simple duplications and deletions in AEXS (5), the molecular basis of inversions remains to be determined. Here, we characterized the fine genomic structures of six rearrangements involved in AEXS. Furthermore, we investigated clinical consequences and local genomic environments of the six rearrangements and of three previously reported duplications/deletions.

Patients and Methods

Patients

This study consisted of six cases (cases 1–6) ascertained by prepubertal- or peripubertal-onset gynecomastia. Clinical findings of cases 1–6 are summarized in Table 1. Cases 1–4 are hitherto unreported. Cases 5 and 6 have been described previously, although the genomic structure remains to be determined (1, 2). Cases 1–3 and 5–6 had a 46,XY karyotype, whereas case 4 had a 46,XY inv (9) karyotype that is known as a normal variant. Case 2 had a brother with prepubertal-onset gynecomastia, a sister with premature thelarche, and a father and several paternal relatives with advanced bone age and/or short stature. Case 6 had a son with prepubertal-onset gynecomastia. There was no family history of AEXS in the remaining cases. This study was approved by the Institutional Review Board Committee at the National Center for Child Health and Development. Written informed consent was obtained from the patients and/or their parents.

Copy-number analyses

Leukocyte genomic DNA samples were obtained from cases 1–6, the parents and siblings of case 2, and the son of case 6. Genomic abnormalities involving *CYP19A1* exons and/or its flanking regions were examined by comparative genomic hybridization (CGH) using a custom-made oligoarray or a catalog human array (4 × 180K format, ID 030700 or G4449A; Agilent Technologies). The procedures were performed as described previously (5).

Department of Molecular Endocrinology (M.F., T.T., D.S., T.O.), National Research Institute for Child Health and Development, 157-8535 Tokyo, Japan; Department of Pediatrics (T.T.), Dokkyo Medical University Koshigaya Hospital, 343-8555 Koshigaya, Japan; Department of Pediatrics and Adolescent Medicine (H.V., M.W.), University Medical Center Ulm, 89081 Ulm, Germany; Metabolism and Cancer Laboratory (K.A.B., H.B., E.R.S.), Prince Henry's Institute, Monash Medical Centre, Clayton, 3168 VIC, Australia; Department of Pediatrics (S.A.), Hakodate Goryoukaku Hospital, 040-8611 Hakodate, Japan; Department of Pediatrics (S.O.), Kitasato University School of Medicine, 252-0375 Kanagawa, Japan; Department of Reproductive Biology (A.U.), Center for Regenerative Medicine, National Institute for Child Health and Development, 157-8535 Tokyo, Japan; Department of Maternal-Fetal Biology (K.N.), National Research Institute for Child Health and Development, 157-8535 Tokyo, Japan; Division of Reproductive Biology Research (S.E.B.), Department of Obstetrics and Gynecology, Feinberg School of Medicine, Northwestern University, Chicago, 60611 Illinois; Department of Reproductive Medicine (M.S.), Graduate School of Medicine, Chiba University, 260-8670 Chiba, Japan; and Department of Pediatrics (T.O.), Hamamatsu University School of Medicine, 431-3192 Hamamatsu, Japan

Table 1. Phenotypic and Endocrine Findings of Cases 1–6

	Case 1	Case 2	Case 3	Case 4	Case 5	Case 6
Genomic rearrangement	Duplication	Deletion	Complex	Complex	Complex	Complex
Age at examination, y	10	8 (18)[a]	15	13	17	36
Phenotypic findings						
Gynecomastia (Tanner stage)	**2–3**	**3**	**4–5**	**3–4**	**Severe**	**Severe**
Onset of gynecomastia, y	**7**	Unknown	**8**	**11**	**7**	**5**
Mastectomy	No	**Yes**	**Yes**	No	**Yes**	**Yes**
Testis, mL	6	N.E.	15	12	Normal	Normal
Pubic hair (Tanner stage)	None	None	3–4	4	N.D.	Normal
Facial hair	None	None	None	Scarce	Scarce	**None**
Final height	Unknown	Unknown	−0.9 SD	Unknown	**<1%ile**	**<1%ile**
Bone age, y[b]	**13.0**	**13.5**	N.E.	**18.0**	N.E.	N.E.
Fertility (spermatogenesis)	Unknown	Unknown	Yes	Unknown	Unknown	Yes
Endocrine findings[c]						
At diagnosis						
LH, mIU/mL	<0.1 (0.4–1.6) → 0.4 (10.9–20.6)[d]		2.4 (1.6–3.5)	1.3 (1.6–3.5) → 24.9 (21.7–39.5)[d]	4.3 (1.4–9.2)	1.7 (1.4–9.2)
FSH, mIU/mL	0.3 (1.7–4.2) → 1.6 (4.6–10.8)[d]		<1.0 (4.2–8.2)	0.6 (4.2–8.2) → 2.1 (11.2–17.3)[d]	2.7 (2.0–8.3)	1.5 (4.2–8.2)
T, ng/mL	0.06 (0.4–1.1) → 3.6 (>2.0)[e]	2.6 (2.8–7.0)	0.7 (2.8–7.0)	1.5 (2.8–7.0)	2.3 (2.8–7.0)	3.2 (2.8–7.0)
E_1, pg/mL				**111** (14–50)	**556** (15–32)	**903** (15–32)
E_2, pg/mL	**14** (<10)	**65** (10–35)	**406** (15–50)	**43** (2–30)	**392** (10–35)	**223** (10–35)
On AI treatment						
LH, mIU/mL	0.5 (0.4–1.6) → 7.3 (10.9–20.6)[d]	**44.8** (0.7–5.7)[f]	**4.7** (1.6–3.5)		8.9 (1.4–9.2)	2.9 (1.4–9.2)
FSH, mIU/mL	1.7 (1.7–4.2)→ 3.2 (4.6–10.8)[d]	**34.9** (2.0–8.3)[f]	2.5 (4.2–8.2)		5.6 (2.0–8.3)	5.6 (4.2–8.2)
T, ng/mL	0.9 (0.4–1.1)	**8.6** (2.8–7.0)	6.9 (2.8–7.0)		5.3 (2.8–7.0)	**10.7** (2.8–7.0)
E_1, pg/mL					**89** (15–32)	27 (15–32)
E_2, pg/mL	<10 (<10)	6 (10–35)	13 (15–50)		**59** (10–35)	**68** (10–35)
Reference	Present study	Present study	Present study	Present study	Ref. 1	Ref. 1

Abbreviations: AI, aromatase inhibitor; E_1, estrone; E_2, estradiol; N.D., not described; N.E., not examined. Abnormal clinical findings are boldfaced. Hormone values below the reference range (shown in parentheses) are underlined, and those above the reference range are boldfaced. Conversion factors to the SI unit: LH, 1.0 (IU/L); FSH, 1.0 (IU/L); E_1, 3.699 (pmol/L); E_2, 3.671 (pmol/L); and T, 3.467 (nmol/L).

[a] Physical examination and endocrine studies were carried out at 8 and 18 years of age, respectively.

[b] Assessed by the Tanner-Whitehouse 2 method standardized for Japanese or by the Greulich-Pyle method constructed for Caucasians.

[c] Evaluated by age-matched male reference data.

[d] GnRH stimulation tests (100 μg/m^2, maximum 100 μg bolus iv; blood sampling at 0, 30, 60, 90, and 120 min).

[e] Human chorionic gonadotropin stimulation tests (3000 IU/m^2, maximum 5000 IU im for 3 consecutive days; blood sampling on d 1 and 4).

[f] Increased levels of LH and FSH during AI treatment may be associated with low E_2 levels (24).

Characterization of the genomic structures of rearrangements

Breakpoints of the rearrangements were determined by direct sequencing of the PCR-amplified DNA fragments harboring the fusion junctions. PCRs were carried out using a number of primer pairs for various genomic positions around *CYP19A1*. The sequences of the primers utilized in the present study are available upon request. To confirm the formation of a chimeric gene in a case with a complex rearrangement, we performed RT-PCR using leukocyte mRNA and primers annealing to exon 2 of *CYP19A1* and exons of neighboring genes. The presence or absence of promoter-associated histone marks in the fused exons was analyzed using the UCSC genome browser (http://genome.ucsc.edu/).

Genotype-phenotype analysis

We performed genotype-phenotype analyses in cases 1–6 and in 18 patients identified in our previous study (*5*).

DNA sequences at the fusion junctions

To clarify the underlying mechanisms of the rearrangements, we examined the presence or absence of microhomologies and short nucleotide stretches at the fusion junctions. In addition, we searched for repeat elements around the breakpoints using Repeatmasker (http://www.repeatmasker.org).

Genomic environments around the breakpoints

We studied the frequencies of known rearrangement-inducing DNA features in the breakpoint-flanking regions. In silico analyses were carried out in the 300-bp regions at the proximal and distal sides of each breakpoint. We also examined control regions (n = 53) randomly selected at an interval of 1.5 Mb from the entire 15q (Supplemental Table 1, published on The Endocrine Society's Journals Online web site at http://jcem.endojournals.org). We calculated the average GC content using GEECEE (http://emboss.bioinformatics.nl/cgi-bin/emboss/geecee) and searched for palindromes using PALINDROME (http://mobyle.pasteur.fr/cgi-bin/portal.py#forms::palindrome) and Non-B structures using Non-B DB (http://nonb.abcc.ncifcrf.gov). Examined Non-B structures included direct repeats, inverted repeats (cruciforms), mirror repeats, A-phased repeats, G-quadruplex repeats, short tandem repeats, and Z-DNA motifs (17). The presence or absence of the 10 specific sequence motifs and two tri/tetranucleotides implicated in rearrangements in various chromosomal regions (14, 18–22) were analyzed using Fuzznuc (http://emboss.bioinformatics.nl/cgi-bin/emboss/fuzznuc).

Replication timing analysis

We analyzed whether the rearrangements at 15q21 have occurred at a specific timing of S phase (23). Replication timing profiles of the approximately 10-Mb genomic interval around *CYP19A1* were evaluated using 92 datasets currently available in

Table 2. Genomic Rearrangements in Cases 1–6

	Rearrangement	Genomic Abnormality	Affected Genes[a]
Case 1	Simple	Simple duplication	*CYP19A1, TNFAIP8L3, AP4E1*
Case 2	Simple	Simple deletion	*CYP19A1, GLDN, DMXL2*
Case 3[b]	Complex	Multiple deletions?	*TMOD3, GLDN, DMXL2?*
Case 4	Complex	Multiple duplications and inversion	*CYP19A1, GLDN, SEMA6D*
Case 5	Complex	Multiple duplications, deletion, and inversion	*TMOD3, DMXL2, TMOD2, LYSMD2, SCG3*
Case 6	Complex	Multiple deletions and inversion	*CGNL1, CYP19A1*

[a] Genes involved in the deletion or duplication. Genes affected by copy-number-neutral inversions are not shown.

[b] Genomic structure of the rearrangement in case 3 remains to be characterized.

the ReplicationDomain database (http://www.replicationdomain.com/replication_timing.php).

Statistical analyses

Statistical significance of the average GC content between the breakpoint-flanking and control regions was analyzed by Student's *t* test. Differences in the frequencies of other rearrangement-inducing DNA features were examined by Fisher's exact probability test. $P < .05$ was considered significant.

Results

Copy-number alterations in cases 1–6

CGH analyses indicated heterozygous genomic rearrangements involving *CYP19A1* and/or its neighboring genes; ie, an approximately 0.4-Mb duplication involving *CYP19A1*, *TNFAIP8L3*, and *AP4E1* in case 1; an approximately 0.3-Mb deletion affecting *DMXL2*, *CYP19A1*, and *GLDN* in case 2; an approximately 80-kb deletion involving *TMOD3* and an approximately 250-kb deletion involving *DMXL2* and *GLDN* in case 3; an approximately 130-kb duplication involving *GLDN* and *CYP19A1* and an approximately 340-kb duplication involving *SEMA6D* at a position of approximately 3.6 Mb distant from *CYP19A1* in case 4; an approximately 370-kb duplication involving *TMOD3*, *TMOD2*, *LYSMD2*, *SCG3*, and *DMXL2*, and a 3- to 35-kb deletion between *DMXL2* and *GLDN* in case 5; and an approximately 3.5-kb deletion in the promoter region of *CYP19A1* in case 6 (Table 2 and Figure 1). The deletion in case 5 could not be narrowed down because of the absence of CGH probes around the breakpoints. The father and siblings of case 2 and the son of case 6 carried the same abnormalities as the probands.

Genomic structures of six rearrangements

We were able to characterize all fusion junctions in cases 1, 2, and 6 and one of the multiple junctions in cases 4 and 5 (Table 3, Supplemental Table 2, and Figure 2). The remaining breakpoints could not be determined due to the low quality of the DNA samples, the presence of long repetitive sequences around the breakpoints, or the complex structures of the rearrangements. In case 1, we identified a 387 622-bp tandem duplication involving six of the 11 exons 1 (exons I.7, 1f, I.2, I.6, I.3, and PII) and all coding exons of *CYP19A1*, together with all exons of *TNFAIP8L3* and *AP4E1*. In case 2, we detected a 303 624-bp deletion involving six of the *CYP19A1* exons 1 (exons I.1, IIa, I.8, I.4, I.5, and I.7), all exons of *GLDN*, and *DMXL2* exons 2–43. In case 4, we identified two duplications: an approximately 130-kb duplication encompassing all noncoding exons 1 and coding exons 2–3 of *CYP19A1* and *GLDN* exon 1, and an approximately 340-kb duplication involving *SEMA6D* exons 1–3. PCR products were obtained with a primer pair for *GLDN* intron 1 and *SEMA6D* intron 3 (P5 and P6 in Figure 2A), indicating that the approximately 3.6-Mb genomic interval harboring *GLDN* exon 1, all noncoding and coding exons of *CYP19A1*, and *SEMA6D* exons 4–20 was inverted. In addition, we analyzed mRNA of case 4 and detected a chimeric clone composed of *CYP19A1* exon 2 and *SEMA6D* noncoding exon 3 (Supplemental Figure 1). Thus, although we could not determine the fusion junctions of the duplication, these data imply that the rearrangement was caused by an inversion of an approximately 3.6-Mb region and a duplication of the telomeric part of the inverted DNA fragment. In case 5, we identified an approximately 370-kb duplication containing *TMOD3* exon 1, *DMXL2* exons 1–29, and all exons of *TMOD2*, *LYSMD2*, and *SCG3*. PCR products were obtained with a primer pair for *TMOD3* intron 1 and the downstream region of *GLDN* (P7 and P8), indicating that the approximately 370-kb region was duplicated and inserted into the genome in a reverse direction. The small deletion between *DMXL2* and *GLDN* detected by CGH could not be characterized because of the presence of long repetitive sequences around the breakpoints. In case 6, we identified a complex deletion–inversion–deletion rearrangement: a 202-bp deletion within *CGNL1* intron 1, an approximately 6.1-Mb inversion encompassing *CGNL1* exon 1, eight of the *CYP19A1* exons 1 (exons I.1, IIa, I.8, I.4, I.5, I.7, 1f, and I.2), and ≥25 genes, and a 3476-bp deletion within *CYP19A1* intron 1.

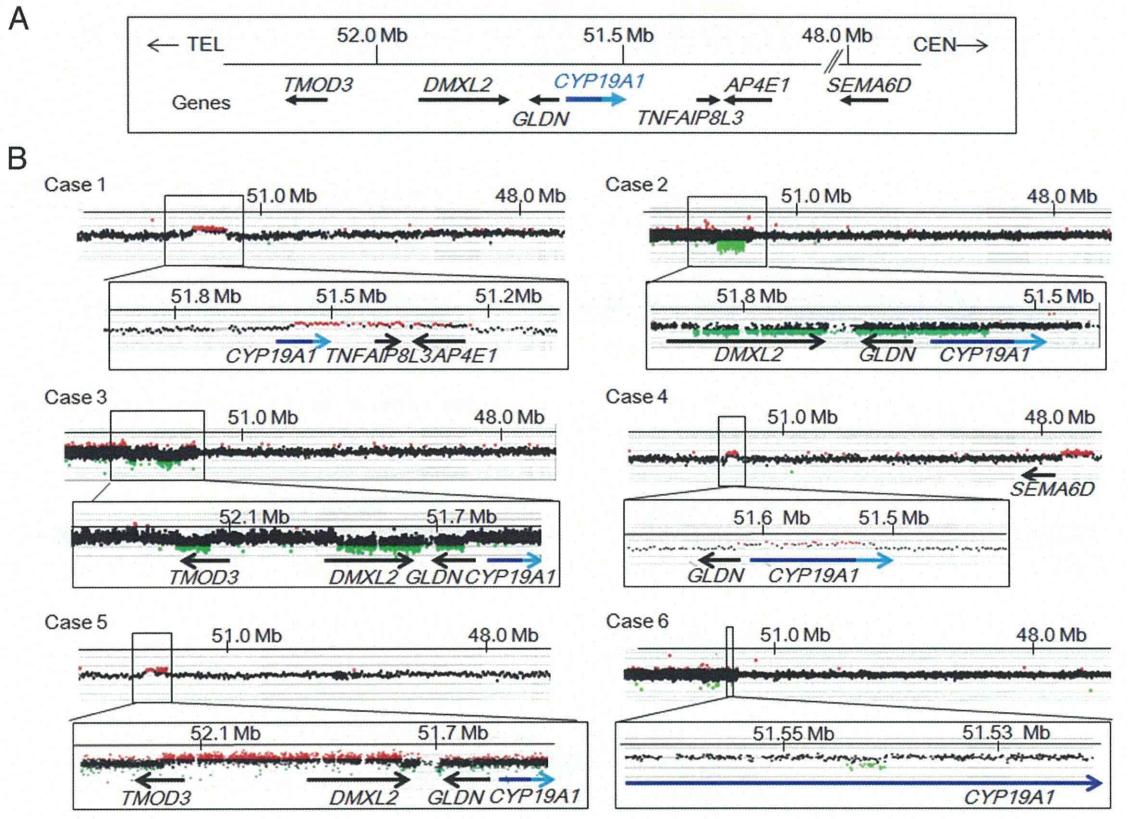

Figure 1. Copy-number analyses in cases 1–6. A, Schematic representation of the normal genomic structure around *CYP19A1*. The arrows indicate genomic positions and transcriptional direction of genes (5′→3′). For *CYP19A1*, the dark and light blue lines denote the genomic regions for noncoding exons 1 and coding exons 2–10, respectively. Genomic positions refer to Human Genome Database (hg19, build 37). Only genes around the fusion junctions are shown. B, CGH analyses in the six cases. The black, red, and green dots denote signals indicative of the normal, increased (>+0.5) and decreased (<−1.0) copy-numbers, respectively.

Phenotypic consequences of the six new and three previously reported rearrangements

We studied genotype-phenotype correlation in cases 1–6 and 18 previously reported patients (four patients from families A–B with simple duplications involving the *CYP19A1* promoter region, and 14 patients from families C–F with *DMXL2-CYP19A1* chimeric genes) (5). The results are summarized in Table 4. First, clinical severities were relatively mild in case 1 and patients from families A–B with simple duplications, obviously severe in cases 5 and 6 with complex rearrangements, and moderate in the remaining cases/patients with simple deletions or complex rearrangements. Second, among cases/patients with simple duplications, case 1 showed earlier onset of gyneco-

Table 3. Fusion Junctions in Cases 1–6

	No. of Fusion Junctions	No. of Fusion Junctions Characterized in This Study[a]	Sequences at the Fusion Junctions		
			Microhomology	Nucleotide Stretch	Predicted Mechanism
Case 1	1	1	Yes (4 bp)	Yes (2 bp)	RBM
Case 2	1	1	Yes (2 bp)	No	RBM
Case 3[b]	2?	0	Unknown	Unknown	RBM?
Case 4	5	1	Yes (20 bp)	No	RBM
Case 5	3	1	Yes (3 bp)	Yes (5 bp)	RBM
Case 6	2	2	Yes (3 bp)[c]/No	No	RBM

Abbreviation: RBM, replication-based mechanism.

[a] Several breakpoints could not be determined due to low quality of the DNA samples, the presence of long repetitive sequences around the breakpoints, or the complex structures of the rearrangements.

[b] Genomic structure of the rearrangement in case 3 remains to be characterized.

[c] Microhomology was observed at the telomeric junction.

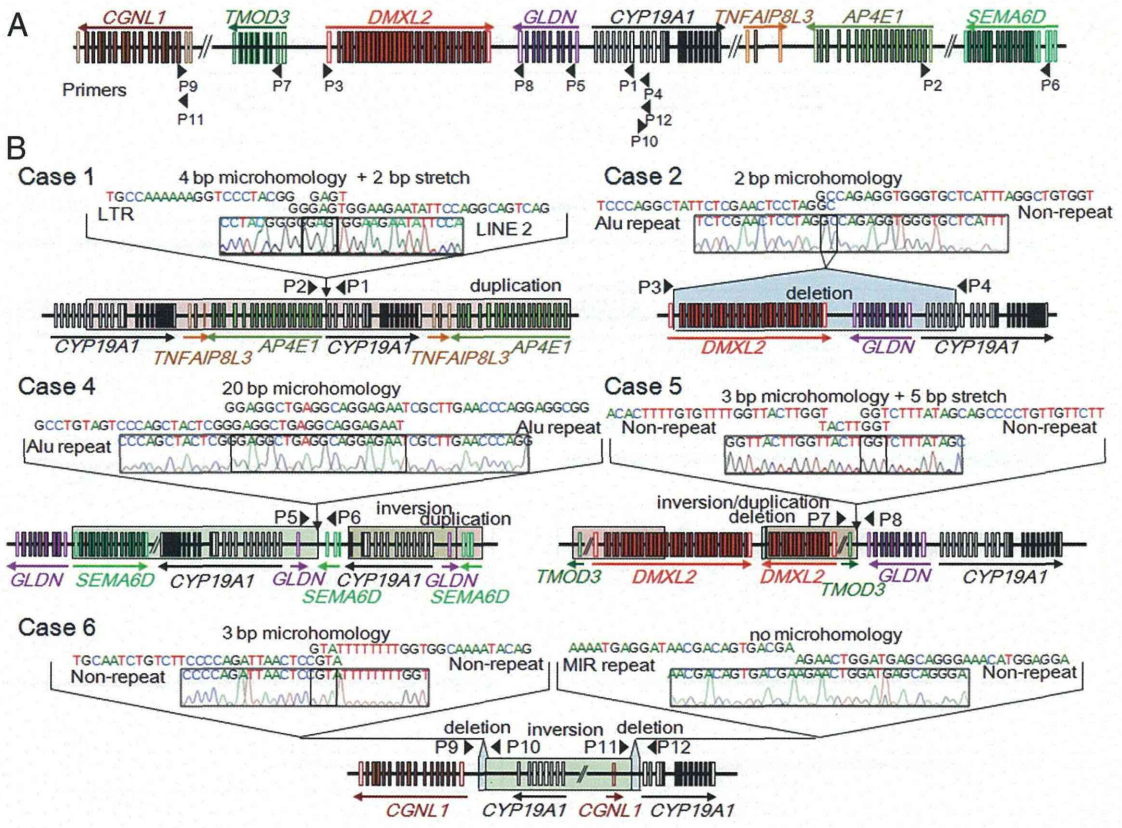

Figure 2. Fine genomic structures of the rearrangements. A, Schematic representation of the normal genomic structure. Arrowheads indicate the positions and the directions (5′→3′) of PCR primers utilized in this study (P1–P12). The open and color-painted boxes denote noncoding and coding exons, respectively. The sizes of the exons, introns, and primers are not drawn to scale. B, Schematic representation of the rearrangements and the DNA sequences at the fusion junctions. The red, blue, and green areas indicate duplications, deletions, and inversions, respectively. P1–P12 indicate the same PCR primers as shown in panel A. The fusion junctions of case 3 were not characterized. For case 4, the precise genomic position of the duplication remains to be clarified.

mastia and more severely advanced bone age than patients from families A–B. Third, among cases/patients with deletions, case 2 manifested milder gynecomastia than case 3 and patients from families C–F. Lastly, among cases/patients with deletions or complex rearrangements, cases 2–4 and patients from families C–F showed milder phenotypes than cases 5 and 6.

DNA sequences at the fusion junctions

We characterized fusion junctions of the rearrangements in cases 1, 2, and 4–6 and in patients from families A–F (Table 3, Supplemental Table 2, and Figure 2). The results indicated the following: 1) nonallelic homologous recombination for the recurrent simple deletions in patients from families D–F that took place between two homologous sequences; 2) nonhomologous end-joining for the nonrecurrent simple deletions in patients from family C that were associated with short nucleotide stretches at the fusion junction; and 3) replication-based mechanisms for the simple and complex aberrations in cases 1, 2, and 4–6, and in patients from families A–B that were accompanied by microhomologies at the fusion junction. Nine of the 18 breakpoints resided within repetitive elements, such as LINE 1, LINE 2, *AluJo*, *AluY*, and *AluSx3*.

Genomic environments around the breakpoints

The average GC content was similar between the breakpoint-flanking and control regions (Supplemental Tables 2 and 3). Furthermore, the frequencies of known rearrangement-inducing DNA features (12, 14, 18–22) did not significantly differ between the breakpoint-flanking and control regions, except for some non-B structures enriched around the breakpoints of the deletions in patients from families D–F (Supplemental Tables 2 and 3).

Replication timing of the 15q21 region

Replication timing analysis indicated that in most cell lines examined, the genomic region around *CYP19A1* is replicated during early S phase (Supplemental Figure 2).

Discussion

We characterized six genomic rearrangements in patients with AEXS (Supplemental Figure 3). In case 1, the tandem duplication seems to have enhanced the transcriptional efficiency of *CYP19A1* in native *CYP19A1*-expressing tissues by increasing the number of transcription start sites. In cases 2–6, the rearrangements are predicted to have

Table 4. Genotype-Phenotype Correlation in Cases 1–6 and Families A–F

Cases/Families[a]	Case 1	Families A and B	Case 2	Case 3[b], Families C–F	Case 4	Case 5	Case 6
Molecular defects							
Predicted mechanism for *CYP19A1* overexpression	Duplication of *CYP19A1* coding exons	Duplication of *CYP19A1* promoters	Chimeric gene formation	Chimeric gene formation	Chimeric gene formation	Chimeric gene formation	Chimeric gene formation
Genes involved in chimeric gene formation	None	None	*DMXL2*	*DMXL2*	*SEMA6D*	*TMOD3*	*CGNL1*
Copy-number of the *CYP19A1* exon 1.4[c]	Normal	Increased	Decreased	Normal	Increased[d]	Normal	Decreased
Clinical findings							
Onset of gynecomastia, y	7	10–13	Unknown	7–12	11	7	5
Gynecomastia (Tanner stage)	2–3	2–3	1–3[e]	3–5	3–4	Severe	Severe
Advanced bone age	Mild	Subtle	Moderate	Mild/ moderate	Severe	N.E.	N.E.

Abbreviation: N.E., not examined.

[a] Cases 1–6 were present cases, whereas families A–F were reported previously (5).

[b] Fine genomic structure of case 3 remains to be characterized.

[c] Exon 1.4 functions as the major promoter in extragonadal tissues.

[d] Duplicated exon 1.4 has been disconnected from the coding exons of *CYP19A1*.

[e] The patient and his father had gynecomastia of Tanner stages 3 and 1, respectively.

created chimeric genes consisting of coding exons of *CYP19A1* and promoter-associated exons of neighboring genes. Actually, the deletions in cases 2 and 3 appear to have permitted splicing between *DMXL2* exon 1 and *CYP19A1* exon 2, as has been shown in the patients with similar deletions (5). Furthermore, the inversion in case 4 was found to produce a chimeric gene consisting of exon 3 of *SEMA6D* and exon 2 of *CYP19A1* (Supplemental Figure 1), and the inversions in cases 5 and 6 have previously been shown to form *TMOD3*- and *CGNL1-CYP19A1* chimeric genes, respectively (2). In this regard, the rearrangements in cases 2–6 have brought not only exons 1 of other genes, but also their flanking regions of >10 kb, to lie near the coding region of *CYP19A1*. Because these flanking regions harbor several enhancer- and promoter-associated histone marks (H3K4Me1 and H3K4Me3) (Supplemental Figure 4), they appear to contain most, if not all, components of cis-regulatory elements. Thus, although we can not examine the actual expression pattern of the chimeric genes, these genes seem to be expressed in a wide range of tissues where the original genes are expressed. These results argue for a broad mutation spectrum of AEXS.

Such diverse genetic basis of AEXS would be relevant to phenotypic variations (Table 4). First, cases/patients with copy-number gains of *CYP19A1* showed milder phenotypes than those with chimeric genes. This is consistent with the limited tissue expression pattern of *CYP19A1* and broad expression patterns of other genes involved in the chimeric gene formation (5, 25). Second, among cases/patients with simple duplications, case 1 showed a more severe phenotype than patients from families A–B. This suggests that tandem duplications encompassing the transcriptional unit, ie, the promoter region plus the coding exons, permit more efficient aromatase protein production than tandem duplications encompassing the promoter region only. Third, among cases/patients with the same *DMXL2-CYP19A1* chimeric gene, case 2 manifested milder phenotypes than case 4 and patients from families C–F. These results can be explained by the difference in the number of *CYP19A1* exons 1, because six of *CYP19A1* exons 1 were deleted in case 2 and all exons 1 were preserved in the remaining cases/patients (Supplemental Figure 5). Fourth, case 4 with a *SEMA6D-CYP19A1* chimeric gene showed a milder phenotype than cases 5 and 6 with a *TMOD3*- and *CGNL1-CYP19A1* chimeric gene, respectively. This is consistent with a tissue expression pattern being broader in *TMOD3* and *CGNL1* than in *SEMA6D* (5, 25). Lastly, cases/patients with *DMXL2-CYP19A1* chimeric genes manifested milder phenotype than cases with a *TMOD3*- or *CGNL1-CYP19A1* chimeric gene. This would primarily be ascribed to the presence or absence of a translational start codon on the fused promoter-associated exons (Supplemental Figure 6). It is likely that *DMXL2-CYP19A1* chimeric mRNAs transcribed by the *DMXL2* promoter preferentially recognize the natural start codon on *DMXL2* exon 1 and undergo nonsense-mediated mRNA decay, and rather exceptional chimeric mRNAs utilize the start codon on *CYP19A1* exon 2 and produce the aromatase protein (5). Such a phenomenon would not be postulated for

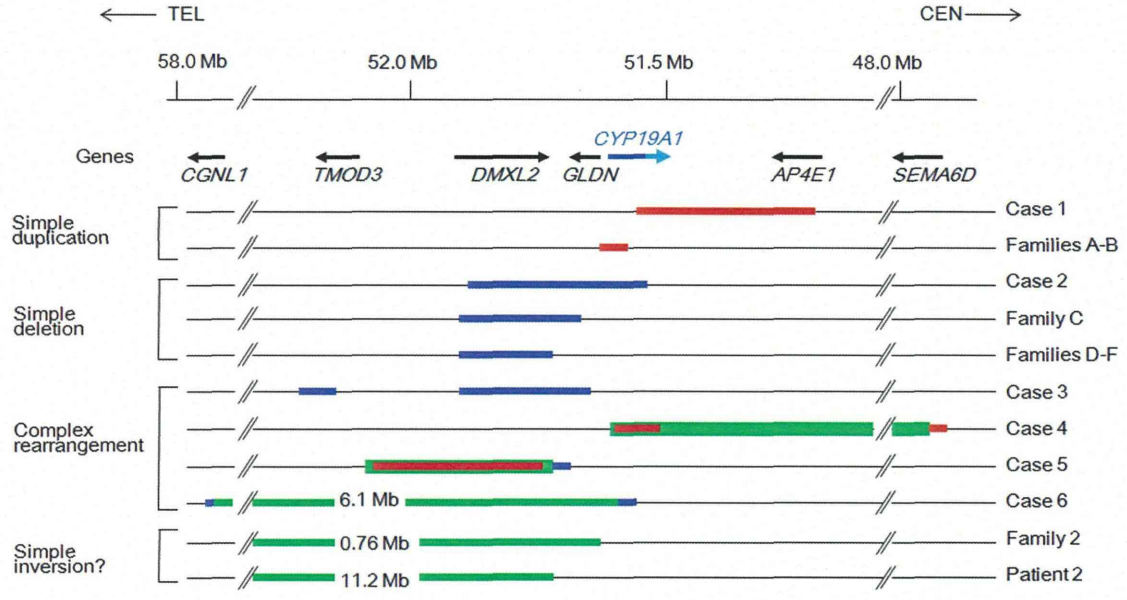

Figure 3. Schematic representation of the 11 rearrangements. Cases 1, 2, and 4–6 are from the present study, and patients from families A–F, patient 2, and patients from family 2 have been reported previously (1, 2, 5). The genomic abnormalities of case 3 were not characterized. The arrows indicate the positions and transcriptional direction of *CYP19A1* and its neighboring genes (5′→3′). Only genes around the fusion junctions are shown. The red, blue, and green lines indicate duplications, deletions, and inversions, respectively. For *CYP19A1*, the dark and light blue lines denote the genomic regions for the noncoding and coding exons, respectively. The inversions of family 2 and patient 2 may be complex rearrangements because copy-number analyses have not been performed in these cases.

the *TMOD3*- and *CGNL1-CYP19A1* chimeric mRNAs because of the absence of a translation start codon on exons 1 of *TMOD3* and *CGNL1*. Taken together, the present study suggests that phenotypic severity is primarily determined by the copy-number of *CYP19A1* and by the expression patterns and structural properties of the fused promoters. It should be pointed out, however, that this conclusion is based on the observation of only a limited number of patients. Phenotypic variation of the patients may be due to low penetrance of the clinical features.

To date, 11 genomic rearrangements have been identified in patients with AEXS (Figure 3). The 11 rearrangements are widely distributed on an approximately 9-Mb region and include simple duplications, deletions, and inversions, as well as complex rearrangements. Of these, the rearrangements in cases 1, 2, and 4–6 and in patients from families A–B are predicted to be replication-based errors (Supplemental Table 2 and Figure 2). Although the short nucleotide stretches at the fusion junctions in cases 1 and 5 may represent "information scars" characteristic of nonhomologous end-joining (9), the complex structures of the rearrangements would be consistent with replication-based mechanisms rather than end-joining (8). However, these rearrangements may result from microhomology-mediated end-joining (26). In contrast, the simple deletions in patients from family C and those in patients from families D–F are compatible with nonhomologous end-joining and nonallelic homologous recombination, respectively (Supplemental Table 2 and Figure 2). These results imply that the genomic region at 15q21 is vulnerable to both recombination- and replication-mediated errors.

In silico analyses revealed that deletions in families D–F due to nonallelic homologous recombination were associated with non-B structures and were located within an early-replicating segment of the genome, whereas the breakpoint-flanking regions of other rearrangements were independent of known rearrangement-inducing DNA features or late-replication timing. These data indicate that there are hitherto unidentified factors that facilitate nonhomologous end-joining and replication-based errors at 15q21. In this regard, it is noteworthy that nine of the 18 breakpoints resided within repetitive elements, and frequencies of *Alu*s (16%) and LINEs (22%) in the breakpoint-flanking regions were slightly higher than expected from the draft human genome (*Alu*, 9.9%; and LINE, 16.1%) (27). An increased number of repetitive sequences was found around the breakpoints of various rearrangements (14, 18, 19, 21), and Boone et al (28) have reported that a high concentration of *Alu* elements may predispose replication-based errors. The presence of various *Alu* family members (*AluJo*, *AluY*, and *AluSx3*) at the fusion junction of our cases supports the notion that moderate sequence similarity between *Alu* elements would be sufficient to provide substrates for replication-based errors (28). Further studies are necessary to clarify the role of repetitive sequences in the formation of rearrangements.

In summary, the present study implies a broad mutation spectrum of AEXS and supports the previously proposed